Nanoelectromechanical Resonator Design and Performance Analysis

T. J. Kouh[*], D. H. Kim[**] and K. L. Ekinci[*]

[*]Aerospace and Mechanical Engineering, Boston University, Boston, MA, USA
[**] School of Mechanical Design and Automation Engineering, Seoul National University of Technology, Seoul 139-743, Korea, dhkim@snut.ac.kr

ABSTRACT

We describe a method for the detection of nanometer scale displacements of nanoelectromechanical resonators. We also present an analysis of the mechanical motion of these devices. We evaluate the effectiveness of the detection technique by detecting displacements from a series of nanomechanical doubly clamped beam resonators with decreasing dimensions.

Keywords: nanoelectromechanical systems, optical interferometry, displacement detection, resonator, fabrication

1. INTRODUCTION

Following the trend in semiconductor electronics, mechanical devices are rapidly being miniaturized into the submicron domain. These nanoelectromechanical systems (NEMS) have dimensions in the deep submicron — mostly operated in their resonant modes. In this size regime, NEMS come with extremely high resonance frequencies, diminished active masses, tolerable force constants and high quality (Q) factors of resonance. These attributes collectively make NEMS suitable for a multitude of technological applications such as ultra-fast actuators, sensors, and high frequency signal processing components.

There exist fundamental and technological challenges to NEMS optimization. One of the remaining challenges to developing technologies based upon NEMS is a robust, sensitive and broadband displacement detection method for sub-nanometer displacements. Most mainstay displacement sensing techniques used in the domain of Microelectromechanical systems (MEMS) are not scaleable into the domain of NEMS — necessitating the development of new techniques to realize the full potential of NEMS. One typical NEMS application is a resonator utilizing a resonant frequency by exciting the device with a same frequency [1-3].

Here, we first describe the fabrication of a NEMS resonator with a fundamental resonance frequency in the tens of MHz. We then describe our optical displacement measurement setup. The setup used is a path-stabilized Michelson interferometer. Finally, we present an analysis of the resonance frequency shift due to the dc electrostatic actuation voltage .

2. EXPERIMENT

Now, we turn to a detailed description of the experimental procedure. We first illustrate the method for fabrication of suspended single crystal silicon structures, and then describe the optical measurements.
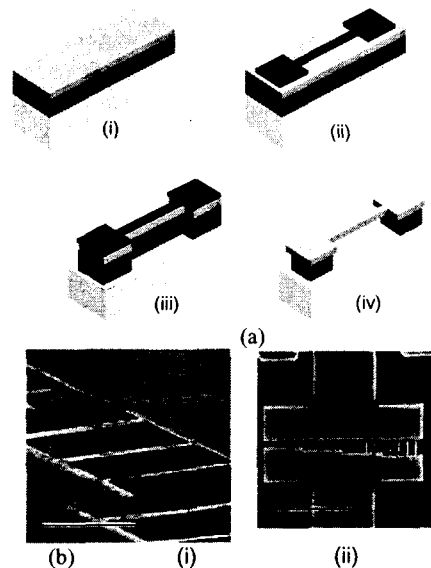

Fig. 1 (a) Surface nanomachining of NEMS. A semiconductor heterostructure with structural (top) and sacrificial (middle) layers on top of a substrate (bottom) is patterned using electron beam lithography and selective etch processes. (b) Scanning electron micrographs of silicon doubly-clamped beams.

The fabrication process is illustrated in Fig. 1 (a). The starting material for device fabrication is a silicon-on-insulator (SOI) wafer with a 219 nm-thick silicon device layer on top of 396-nm-thick oxide layer. Fabrication begins by defining large area contact pads by optical lithography. A 40-nm-thick layer of Cr is then evaporated and, subsequently, standard liftoff is carried out with acetone. Samples are then coated with a bi-layer PMMA (polymethyl methacrylate) resist prior to patterning by electron beam lithography. After resist exposure and development, 40 nm of Cr is evaporated on the samples, followed by liftoff in acetone. The pattern in the Cr metal mask is then transferred to the oxide layer beneath it by

anisotropic reactive ion etching (RIE). We use a plasma of CF_4 and O_2 at a pressure of 300 mTorr with respective flow rates of 50 sccm and 5 sccm, and a microwave power of 300 W. The etch rate under these conditions is ~6 nm/s. The vertically-etched structures are then released by a controlled selective isotropic etching of the underlying oxide layer using hydrofluoric acid (HF). Fig. 1 (b) shows scanning electron micrographs of completed NEMS devices.
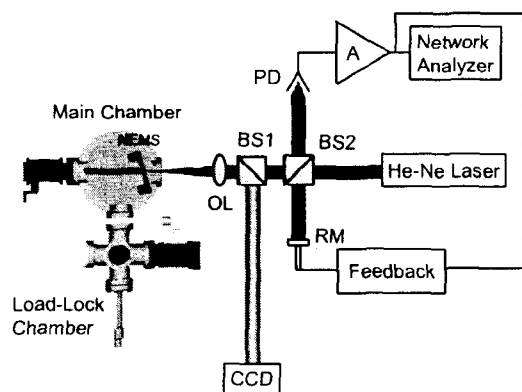
The measurements on fabricated devices are carried out inside an ultrahigh vacuum (UHV) chamber using a path stabilized optical interferometer. The block diagram of this set up is displayed in Fig. 2 (a). After fabrication, the devices are introduced into the main chamber through a load lock and transferred onto a single-axis linear translator. The motion of the translator brings the devices towards an optical view-port as shown in the Fig. 2 (b) — allowing probing of the devices by a laser beam.

The whole optical interferometer is mounted on a XYZ translation stage. The interferometer comprises various beam-splitters (BS), a reference mirror (RM) and a photo-detector (PD) as shown in Fig. 2 (a). Coherent light from a He-Ne laser with wavelength, $\lambda \approx 635$ nm is split into two beams — the first beam traveling along a reference path and a second beam used as a probe for NEMS displacement detection. A feedback circuit and a mirror mounted on a

piezoelectric actuator control the length of the reference path. The probe beam used for NEMS displacement detection is focused on the device by a 50X objective lens (OL) with numerical aperture, $NA=0.5$. The light reflected from the NEMS is collected by the same lens.

The probe beam reflected from the NEMS device and the beam in the reference path form an interference pattern on the photodetector. The optical path length that the probe beam travels and consequently, the intensity of the interference pattern on the photodetector change as the NEMS device displaces out of plane (in the z-direction). The intensity variations on the photodetector are measured by a network analyzer.

The NEMS devices are actuated electrostatically [4] and their displacements are detected using a network analyzer as shown in Fig. 2 (c). Fig. 3 shows the UHV chamber and optics measurement setup where all are placed on an air-pressure controlled mounting plate.

(a)   (b)
Fig. 3 (a) nano resonator in UHV chamber (b) Optics mesurement setip

3. ANALYSIS OF THE RESONANCE FREQUENCY SHIFT IN ELECTROSTATIC ACTUATION

Here, we present an analysis of the mechanical vibrations of a double clamped nanomechanical beam. We use an elastic continuum analysis of a thin beam (Fig. 4). The out of plane (z-direction) equation of motion of the beam is

$$\frac{\partial^4 z}{\partial x^4} = -\frac{\rho A}{EI}\frac{\partial^2 z}{\partial t^2} + \frac{F_e(z,t)}{EI} \qquad (1)$$

where E is Young's modulus, A is the beam's cross sectional area, ρ is its mass density. $F_e(z,t)$ is the applied force per unit length in the x-direction, which will be addressed in detail. I is the moment of area of the beam, which is evaluated as $AT^2/12$ when the beam has a rectangular cross section and thickness of t.

Solution of the beam equation can be obtained by separation of variables:

$$z(x,t) = e^{-i\omega_n t}(\alpha_1 e^{-i\lambda_n x} + \alpha_2 e^{i\lambda_n x} + \alpha_3 e^{-i\lambda_n x} + \alpha_4 e^{i\lambda_n x}) \qquad (2)$$

(a)

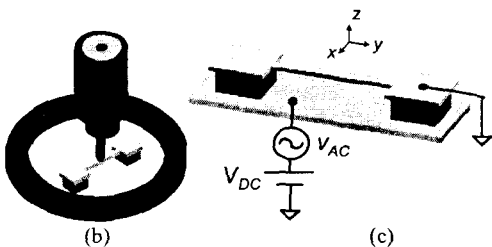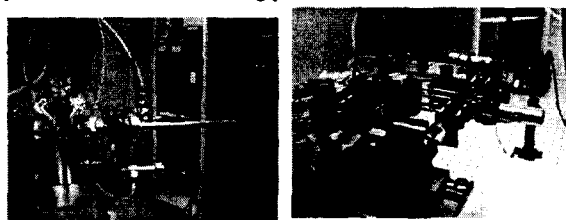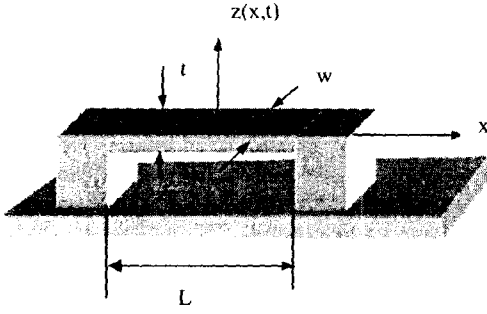(b)   (c)

Fig. 2 (a) Schematic diagram of the optical measurement setup and the UHV chamber. (b) Close up of the NEMS device in the vicinity of the quartz optical view-port. (c) Schematic diagram of the electrostatic actuation.

$$z(x,t)$$

Fig. 4 Transverse motion of double clamped nano beam

where λ_n is the wave number and is determined from the boundary conditions, and n is an index representing a particular mode of vibration. ω_n is the angular velocity for mode n. For a clamped beam at both ends, the frequencies of normal modes are obtained by [5]

$$f_n = C_n \frac{t}{L^2} \sqrt{\frac{E}{\rho}} \qquad (3)$$

The coefficients for the first three modes are given as $C_1 = 1.03$, $C_2 = 2.83$, and $C_3 = 5.55$, respectively.

Next, we turn to the time component of the equation of motion. The beam can be modeled as a lumped system with a single degree of freedom:

$$m\ddot{z} + b\dot{z} + kz = -Fe \qquad (4)$$

where m is the beam mass, b is the damping coefficient, which is related to the quality factor, and k is the beam stiffness. In electrostatic excitation, the force is due to the attractive forces between the plates of a capacitor. We can compute the force, F_e, exerted on the upper plate due to an applied voltage V as

$$Fe = -\frac{1}{2} \frac{\varepsilon_r \varepsilon_0 wL}{(d-z)^2} V^2 \qquad (5)$$

where ε_0 is the permittivity of free space, with $\varepsilon_0 = 8.85*10^{-12} \, C^2/N\text{-}m^2$, and ε_r is the relative permittivity, and d is the initial gap.

Substituting the electrostatic force in the dynamic equation, we obtain

$$m\ddot{z} + b\dot{z} + kz = -Fe = \frac{1}{2} \frac{\varepsilon V^2}{(d-z)^2} \qquad (6)$$

Here, we define a new constant, $\varepsilon = \varepsilon_r \varepsilon_0 wL$. Assuming that the displacement, z, is small, we can linearize the above equation around an operating point. Then, the right side of (6) can be written by Taylor series expansion:

$$f(z) = \frac{1}{(d-z)^2} = f(0,0) + \frac{\partial f}{\partial z}\Big|_{z=0} z + ... = \frac{1}{z^2} z - \frac{2}{d^3} z + ... \qquad (7)$$

Keeping the large terms in the expansion, we obtain

$$m\ddot{z} + b\dot{z} + kz = \frac{1}{2}(\frac{1}{d^2} + \frac{2}{d^3} z)\varepsilon V^2 \cdot \qquad (8)$$

Finally,

$$m\ddot{z} + b\dot{z} + (k - \frac{\varepsilon V^2}{d^3})z = \frac{1}{2d^2}\varepsilon V^2 \cdot \qquad (9)$$

We observe that the effective spring constant of the system is affected by the external excitation voltage. Therefore, given the natural frequency of the free vibrations, $\omega_0 = \frac{k}{m}$, the frequency of the excited system will be

$$\omega^2 = \frac{(k - \frac{\varepsilon V^2}{d^3})}{m} = \frac{k}{m} - \frac{\varepsilon V^2}{md^3} = \omega_0^2 - \frac{\omega_0^2}{k}(\frac{\varepsilon V^2}{d^3}) \qquad (10)$$

$$= \omega_0^2 (1 - \frac{\varepsilon V^2}{kd^3})$$

In the experiments, on usually uses an ac and dc excitation voltage:

$$V = V_{DC} + V_{AC} \sin \omega t \qquad (11)$$

or

$$V^2 = V_{DC}^2 + 2V_{DC}V_{AC} \sin \omega t + \frac{V_{AC}^2(1 - \cos 2\omega t)}{2} \qquad (12)$$

Since the resonance frequency depends on V^2, which includes a $\cos 2\omega t$ term, the stiffness has a parametric quality, i.e., the system will possess a parametric resonance. To analyze this phenomena in some more detail, we introduce an average fundamental frequency, $\bar{\omega}$, measured over a period of the resonance cycle, T, as

$$\bar{\omega}^2 = \omega_0^2 - \omega_0^2 (\frac{\varepsilon}{kd^3}) \frac{1}{T} \int_0^T V^2 dt$$

$$= \omega_0^2 \left[1 - (\frac{\varepsilon}{kd^3})(V_{DC}^2 + \frac{V_{AC}^2}{2}) \right] \qquad (13)$$

The concept of the average fundamental frequency is beneficial when we consider a rough estimation for the beam system. Evidently, the average resonance frequency shifts with both the ac and the dc voltage.

4. EXPERIMENTAL RESULTS

Fig. 5 shows the out-of-plane fundamental resonance frequencies of a family of doubly-clamped silicon beams, with rectangular cross sections and different aspect ratios (length/width). The beams are 10 μm long and 200 nm thick with widths of 1000 nm, 750 nm, 500 nm and 250 nm. There is a metallization layer of 1 nm Cr and 1.5 nm Au atop the beams. This particular family of devices yields out-of-plane resonant frequencies between 16.5 MHz and 17.1 MHz. Quality (Q) factors [6] measured were in the range 300<Q<3000 at room temperature.
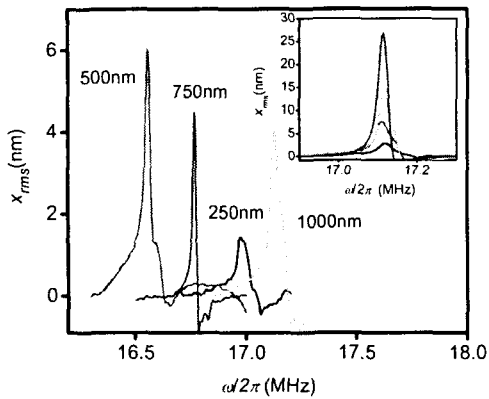
Fig. 5 Frequency spectrum of four suspended silicon beams of 10 μm-long (L) and 200 nm-thick (t) with different widths (w) of 1000 nm, 750 nm, 500 nm and 250 nm.

The fundamental resonance frequency, $\omega_0 / 2\pi$, of a doubly-clamped beam of length, L, and thickness, t, varies linearly with the geometric factor t/L^2 according to the simple relation $\omega_0 / 2\pi = 1.03(\sqrt{E/\rho})t/L^2$ where E is the Young's modulus and ρ is the mass density. The measured frequencies are within 4% of the theoretical predictions (Fig. 6). In principle, the beam width does not depend on the resonant frequency, however, the frequency is changed without any trend. This mainly occurs because the laser beam spot size (630 nm) is bigger than the beam width or close to the spot size, the light has a diffraction from the substrate. It actually weakens the true signal that we want to detect.

The inset shows the frequency spectrum of the silicon beam of 10 μm × 200 nm × 1000 nm as a function of DC driving amplitude, V_{DC}. The lowest curve corresponds to 1 V and V_{DC} is increased by 1V at fixed AC voltage of 800mV. All the measurements are done at 2×10^{-9} Torr.

With increasing V_{DC}, the beam is driven into larger rms amplitude as described above. Also, increasing V_{DC}, resonance frequency is shifted to the less value (Fig. 7), which agrees with the theoretical result shown in previous section.
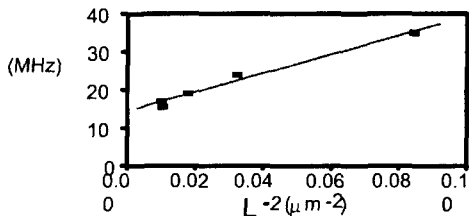

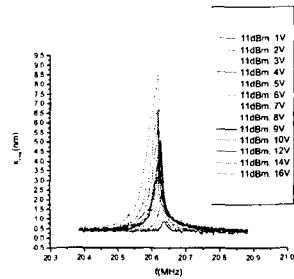Fig. 6 Resonance frequency shift due to beam length variations

Fig. 7 Resonance frequency shift due to DC voltage variations

5. CONCLUSIONS

We have presented an experimental study and a theoretical analysis of NEMS device motion. We measured out of plane fundamental resonances of silicon NEMS with dimensions as small as 10 μm × 200 nm × 1000 nm in UHV at room temperature. The resonant frequencies were ~17MHz and the quality factors were in the range $300<Q<3000$. Resonant frequencies were adjustable by the application of dc and ac voltages.

REFERENCES

[1] D. W. Carr and H. G. Craighead , J. Vac. Sci. Technol. B 15, 2760, 1997.
[2] L. Sekaric, D.W. Carr, S.Evoy, J.M. Parpi, H.G. Craighead, Seosors ans Actuators A 101, 215, 2002.
[3] A. N. Cleland, M. L. Roukes, Applied Physics Letters 69, 2653, 1996.
[4] T.R. Albrecht, P. Grütter, D. Rugar, D.P.E. Smith, Ultramicroscopy 42, 1638, 1992.
[5] L. Sekaric, J.M. Parpi, H.G. Craighead,T. Feygelson, B.H. Houston, J.E. Butler, Applied Physics Letters 81, 4455, 2002.
[6] A.N. Cleland, "Foundations of Nanomechanics", Springer, 2003.